Competition among the decay modes of projectile remnants in (600 MeV/nucleon) Au + Cu reactions

Wang Fei,[2] Sa Ben-Hao,[1–3] Zheng Yu-Ming,[1,2] and Zhang Xiao-Ze[2]
[1]*CCAST (World Laboratory), P. O. Box 8730, Beijing 100080, China*
[2]*China Institute of Atomic Energy, P.O. Box 275(18), Beijing 102413, China*
[3]*Institute of Theoretical Physics, Academia Sinica, Beijing, China*
(Received 6 September 1995)

The relative yield of decay modes of a projectile remnant as a function of $\langle Z_{\rm bound}\rangle$ has been analyzed from the ALADIN data of (600 MeV/nucleon) Au + Cu, and it is consistent with the corresponding theoretical results of the incomplete-fusion-fragmentation model. The experimental and theoretical results of the relative yield of decay modes and of the Campi plot and the theoretical results of the thermodynamical temperature plot show nicely the competition and transformation processes of the decay modes of the projectile remnant with the decreasing of $\langle Z_{\rm bound}\rangle$. [S0556-2813(96)00407-4]

PACS number(s): 25.70.Pq, 24.60.Ky, 25.70.Mn

I. INTRODUCTION

A nuclear system has the character of a short-range repulsive and longer-range attractive force, which shows typical van der Waals behavior as in molecular dynamics and encourages the investigations of a liquid-gas phase transition both theoretically and experimentally [1–10].

Later on the studies were extended to the disassembly of a hot nucleus in medium-energy nucleus-nucleus collisions [9–18]. In [11], a peak structure at thermodynamical temperature $T\sim$ 5 MeV was found in the curve of heat capacity versus thermodynamical temperature resulting from the canonical Monte Carlo simulation for the disassembly of a hot nucleus ^{238}U*. The backbending phenomenon (or the temperature plateau) at $T\sim$ 5 MeV in the plot of thermodynamical temperature as the function of excitation energy per nucleon (T versus ϵ^*) was then discovered for the disassembly of an ideal hot nucleus ($A_h=100$ and $Z_h=50$) using the Copenhagen statistical multifragmentation model [12]. Sequentially, a similar temperature backbending at $T\sim$ 5 MeV in the microcanonical Monte Carlo simulation of the disassembly of a hot nucleus ^{131}Xe* was reported in [13,14]. In [13,14] the second temperature backbending at $T\sim$ 6 MeV was discovered as well. These two backbendings were explained, as corresponding to the changing-over of the dominant decay mode of the hot nucleus from the pseudoevaporation mode to the pseudoevaporation plus pseudofission modes and to the multifragmentation mode, respectively [13,14]. These transformations were named as decay mode transformations of the hot nucleus. The temperature plateau above has been proved preliminarily by the experiment [18].

In [13,14,16,17] the mass number of the referential fragment ($A_r\leqslant A_h/10$) was introduced, according to which the definition of decay modes for a hot nucleus is given: The pseudoevaporation mode (E) refers to the decay event of the hot nucleus in which there is only one fragment with $A_f\geqslant A_r$ and the rest are smaller. The decay event of the hot nucleus with only two fragments A_{f1} and $A_{f2}\geqslant A_r$ is defined as the pseudofission mode (F). The multifragmentaion mode (M) stands for the event in which there are at least three fragments A_{f1}, A_{f2}, and $A_{f3}\geqslant A_r$. An event composed of an assembly of protons, neutrons, and light fragments with mass number $A_f<5$ is named as the vaporization mode (V). The results of the relative yield of decay modes as a function of excitation energy of the hot nucleus, ^{131}Xe*, confirmed nicely the decay mode transformation [13,14], mentioned above.

Recently published ALADIN data of correlations among the charges of fragments emitted from the projectile remnant in reactions of a (600 MeV/nucleon) Au projectile on different targets (C, Al, Cu, and Pb) [19–21] support strongly the establishment of the thermal equilibrium in the fragmenting nucleus (hot nucleus) before breakup. That has attracted great interest among theorists. These correlations include the mean multiplicity of IMF's ($3\leqslant Z_{\rm IMF}\leqslant 30$), the average charge of the largest fragment ($Z_{\rm max}$), the ratio of charge moments (γ_2), the asymmetry of the largest to second largest charge (a_{12}), and the three-body asymmetry (a_{123}) as a function of the $Z_{\rm bound}$ (which is the sum of the charges of fragments with $Z_f\geqslant 2$ and is a measurement of the violence of the collision). A lot of successful theoretical explanations by using the statistical model or the combination of dynamical and statistical calculations or the combination of dynamics and percolation calculations have been published [21–25]. Recently we have also reproduced satisfactorily the ALADIN data of (600 MeV/nucleon) Au + Cu reactions using the incomplete-fusion-fragmentation model (IFFM) [26].

In this paper we give the results of the relative yield of the decay modes as a function of $\langle Z_{\rm bound}\rangle$, analyzed from the ALADIN data of the projectile remnant in the reaction (600 MeV/nucleon) Au + Cu and the corresponding theoretical results of IFFM. For comparison we give also the Campi plot, both analyzed from the data and calculated with IFFM, and the theoretical plot of thermodynamical temperature versus excitation energy per nucleon. The theoretical results are all comparable with the corresponding experiments. All the experimental results indicate consistently that the ALADIN data do really imply the messages of the competition among the decay modes of the projectile remnant and the transfor-

mation of the decay modes from each other. The analysis of the relative yield of the decay modes is a much better way than the Campi plot, etc., in studying the competition and transformation of decay modes.

II. BRIEF REVIEW OF THE INCOMPLETE-FUSION-FRAGMENTATION MODEL

The proposed incomplete-fusion-fragmentation model [27–30,26] is a hybrid dynamical-statistical model. In IFFM, the formation of a hot nucleus is depicted as an incomplete-fusion process. The projectile remnant (one of the hot nuclei) is composed of projectile nucleons outside the overlapping region between the target and projectile nuclei under a given impact parameter. The target nucleons and the remains of projectile nucleons form the target remnant (another hot nucleus). The number of projectile nucleons inside the overlapping region is calculated according to the collision geometry (or participant-spectator model). If one assumes that the ratio of the charge number to mass number of the projectile remnant is equal to the corresponding ratio of the projectile nucleus, as in [21–26], the mass and charge numbers of the projectile and target remnants are then decided. Since the incident energy is quite high in comparison with the energy of the Fermi motion and/or the energy of the nucleon interaction, it is reasonable to assume that in the initial stage of reaction the spectator projectile nucleons escape as a whole (projectile remnant) with beam velocity. The reaction energy Q can then be calculated in virtue of mass balance. From the energy and momentum conservations, the kinetic energy deposited in the reaction system (projectile and target remnants) can be calculated. The sum of the reaction energy and the deposited energy is regarded as the available reaction energy. This available reaction energy is shared among the projectile and target remnant nucleons with different weight parameters of f_P and $f_T=1+(1-f_P)(A_P/A_T)$, respectively. The excitation energy of the projectile remnant is assumed to be a part of its available reaction energy and the corresponding fractional factor is regarded as a model parameter. The other part is consumed in the process approaching thermal equilibrium (freezeout). We refer to [27–30,26] for details.

The statistical multifragmentation model (Berlin-Beijing model) [11,31,13,14,32] is then used to describe the disassembly of the projectile remnant at freezeout. In this model it is assumed that the projectile remnant (hot nucleus) disassembles promptly into a configuration described by a set of variables $\{N_c,\ N_n,\ \{A_i,\ Z_i\}_{i=1}^{N_c},\ \{\vec{r}_i\}_1^{N_c},\ \{\vec{p}_i\}_1^{N_c},\ \{\epsilon_i\}_1^{N_c},\ \{\vec{r}_j\}_1^{N_n},\ \{\vec{p}_j\}_1^{N_n}\}$. Here N_c refers to the number of charged fragments including prompt protons. N_n stands for the number of prompt and evaporated neutrons. $\{A_i,\ Z_i\}_{i=1}^{N_c}$, $\{\vec{r}_i\}_1^{N_c}$, $\{\vec{p}_i\}_1^{N_c}$, and $\{\epsilon_i\}_1^{N_c}$ are the set of mass and charge numbers, position, momentum, and internal excitation energy of charged fragments. $\{\vec{r}_j\}_1^{N_n}$ and $\{\vec{p}_j\}_1^{N_n}$ are the set of position and momentum of neutrons. The configurations allowed by the mass, charge, momentum and energy conservations are assumed to conform to a distribution of canonical or microcanonical ensemble. By means of the Monte Carlo method and the corresponding Metropolis pass a large number of allowed configurations (10^6, say) are generate. The physical observables can then be calculated as a statistical average.

TABLE I. The characteristics of the projectile remnant in the reaction (600 MeV/nucleon) Au + Cu calculated from the incomplete-fusion-fragmentation model.

b (fm)	A_P	Z_P	E^* (MeV)	ε^* (MeV/nucleon)	$\langle Z_{\rm bound}\rangle$
1	67	27	373.8	5.58	24.3
2	74	30	405.5	5.48	27.1
3	89	36	465.3	5.23	32.2
4	107	43	523.0	4.90	38.4
5	125	50	554.5	4.44	44.6
6	143	57	549.1	3.84	50.8
7	159	64	497.8	3.13	57.2
8	173	69	402.7	2.33	63.9
9	184	74	261.8	1.42	70.8
10	192	77	117.2	0.61	76.6

III. RESULTS AND DISCUSSIONS

Table I gives the mass number A_h, the charge number Z_h, the excitation energy E_h^* (ϵ^* in addition) and the averaged $Z_{\rm bound}$ of the projectile remnant in reaction (600 MeV/nucleon) Au + Cu, calculated with IFFM. Since in the theoretical calculation there is a distribution of $Z_{\rm bound}$ (in a small interval) and a corresponding $\langle Z_{\rm bound}\rangle$ for each projectile remnant, in order to compare theory with experiment rigorously the same $Z_{\rm bound}$ interval is used to analyze ALADIN data instead of the constant bin in [21].

The relative yield of decay modes of the projectile remnant as a function of $\langle Z_{\rm bound}\rangle$ is given in Fig. 1 for the reaction (600 MeV/nucleon) Au + Cu: Fig. 1(a) is the ALADIN data and Fig. 1(b) is the results of IFFM. Since the ALADIN data are the charge distribution of fragments here we use the charge number of the referential fragment Z_r,

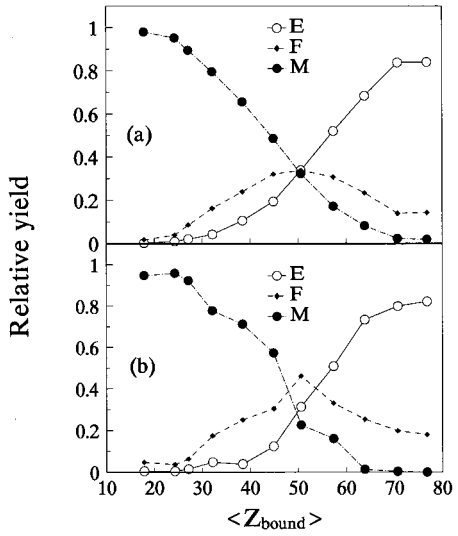

FIG. 1. Relative yield of decay modes as a function of $\langle Z_{\rm bound}\rangle$ for the projectile remnant in the reaction (600 MeV/nucleon) Au + Cu: (a) ALADIN data, (b) results of IFFM.

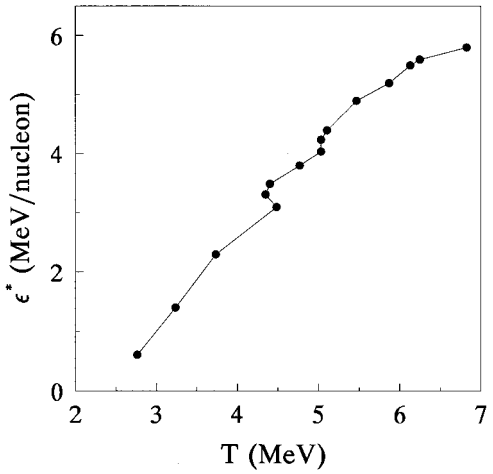

FIG. 2. Thermodynamic temperature as a function of excitation energy per nucleon for the projectile remnant in the reaction (600 MeV/nucleon) Au + Cu.

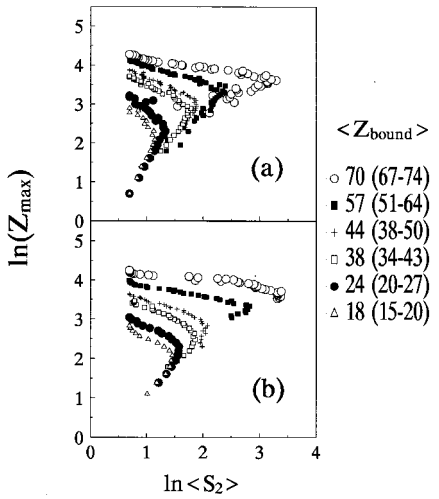

FIG. 3. The Campi plot for the projectile remnant in the reaction (600 MeV/nucleon) Au + Cu: (a) ALADIN data, (b) results of IFFM.

$$Z_r = \frac{Z_h}{C}, \tag{1}$$

to define the decay mode instead of the mass number of referential fragment in [13,14,16,17]. In Eq. (1), the constant C is equal to 12.8. When the value of Z_r given by Eq. (1) is real the results in Fig. 1 are the averaged results over the integers $Z_r \pm 1$. One learns from Fig. 1(a) that the E mode is dominant at very large $\langle Z_{\text{bound}} \rangle$ (very peripheral collisions) where the F mode is small and no M mode at all. With the decreasing of $\langle Z_{\text{bound}} \rangle$, i.e., increasing of centrality, the relative yield of the E mode decreases rapidly, the yield of the F mode increases and shares the percentage together with the E mode. If $\langle Z_{\text{bound}} \rangle$ decreases further, the M mode appears, grows quickly, and becomes dominant at a very central collision, where the E mode disappears and the F mode is smaller. The consistency between experimental and theoretical results is very well.

The thermodynamical temperature as a function of excitation energy per nucleon resulted from IFFM for the projectile remnant in the reaction (600 MeV/nucleon) Au + Cu is given in Fig. 2. Two temperature backbendings appear in Fig. 2, one is located at $T \sim$ 4.5 MeV and another at $\sim$ 5.1 MeV. In comparison with Fig. 1 and noticing Table I one can see that the first temperature backbending (at $\epsilon^* \sim 3$ MeV) just corresponds to the place where the E mode drops down rapidly in Fig. 1 and therefore corresponds to the transformation from the E mode dominance to $E+F$ mode dominance. The second temperature backbending (at $\epsilon^* \sim 4.5$ MeV) corresponds to the place where the M mode grows up quickly, i.e., to the transformation to the M mode dominance.

The Campi plot, i.e., the plot of $\ln Z_{\max}$ versus $\ln\langle S_2 \rangle$ is given in Fig. 3. Figures 3(a) and 3(b) are the results of ALADIN data and IFFM, respectively. Here S_2 refers to the second-rank conditional moment [33]

$$S_2 = \frac{M_2}{M_1}, \tag{2}$$

and

$$M_k = \sum_i Z_i^k, \tag{3}$$

where M_k stands for the kth-rank moment in a single event and the sum is running over all fragments except the heaviest one. As for $\langle S_2 \rangle$, it is the averaged S_2 over the events with the same $Z_{\max}$. The Campi plot had been thought of as the remnant of critical phenomena in the disassembly of the hot nucleus [33,34]. The events falling on upper and lower branches are attributed to the E and/or F mode events and to the M mode events, respectively, the cross point of those two branches is regarded as the critical point. Although it was pointed out in [35] that the Campi plot is not a sufficient condition for the decay mode transformation of the hot nucleus, it is worthwhile to have the Campi plot in comparing with others. Figure 3 indicates that as the collision centrality decreases ($\langle Z_{\text{bound}} \rangle$ increases), the number of events falling on the lower branch decreases, the absolute slops of both branches decrease, the zone of the lower branch shrinks, and the values of $Z_{\max}$ and $\langle S_2 \rangle$ increase. When $\langle Z_{\text{bound}} \rangle$ is large enough, most of the events fall on the upper branch, there are only few points on the lower branch, and the absolute slops of both branches approach zero. The agreement between theoretical and experimental Campi plots here is quite good and is even better than that in [36]. The more interesting thing is that the Campi plot shows the same rule for the competition and transformation of decay modes as the ones shown in other figures, mentioned above.

It is worthwhile to point out that the vaporization decay mode of the projectile remnant has not been shown in Fig. 1. It might indicate that the excitation energy per nucleon needed for the onset of the vaporization decay mode (i.e., the

liquid-gas phase transition [15,37]) is beyond the region in question. The saturation of the excitation energy per nucleon with decreasing of $\langle Z_{\rm bound}\rangle$ sets a limit to the multifragmentation mode and prevents the appearance of the vaporization decay mode (liquid-gas phase transition).

IV. SUMMATION

In summary, we have analyzed the relative yields of decay modes for the projectile remnant in reaction (600 MeV/nucleon) Au + Cu and compared them with the corresponding results of IFFM. The Campi plot, both analyzed from ALADIN data and calculated by IFFM, and the calculated thermodynamical temperature plot are also given here. Not only do all the theoretical results agree reasonably with corresponding experimental ones but they also show the competition and transformation processes of decay modes of the projectile remnant consistently and satisfactorily.

Note added. After the submission of our paper, we heard at INPC '95 in Beijing that the ALADIN/LAND collaboration has analyzed the experimental plot of temperature versus excitation energy per nucleon for the projectile remnant in the Au + Au collision at 600 MeV/nucleon. A temperature plateau at $T\sim 4.5-5$ MeV is observed [38], which is consistent with the results of IFFM here (cf. Fig. 2). As for the zone of temperature backbendings at the ϵ^* axis in the results of IFFM is much narrow than the data, it is because of the reaction system here is Au + Cu and that here one is limited to the study of the multifragmentation decay mode and assumes the saturation of excitation energy with decreasing of $\langle Z_{\rm bound}\rangle$.

ACKNOWLEDGMENTS

We thank W. Trautmann for supplying the ALADIN data. Thanks also go to D. H. E. Gross and B-A. Li for discussions. This work was supported by the National Natural Science Foundation of China.

[1] D. Q. Lamb, J. M. Lattimer, C. J. Pethick, and D. G. Ravenhall, Phys. Rev. Lett. **41**, 1623 (1978).
[2] P. J. Siemens, Nature **305**, 410 (1983).
[3] H. Schulz, D. N. Voskresensky, and J. Bondorf, Phys. Lett. **133B**, 141 (1983).
[4] G. Bertsch and P. J. Siemens, Phys. Lett. **126B**, 9 (1983).
[5] M. W. Curtin, H. Toki, and D. K. Scott, Phys. Lett. **123B**, 289 (1983).
[6] H. Jaqaman, A. Z. Mekjian, and L. Zamick, Phys. Rev. C **27**, 2782 (1983).
[7] P. Bonche, S. Levit, and D. Vautherin, Nucl. Phys. **A436**, 265 (1985).
[8] S. Levit and P. Bonche, Nucl. Phys. **A437**, 426 (1985).
[9] J. E. Finn, S. Agarwal, A. Bujak, J. Chuang, L. J. Gutay, A. S. Hirsch, R. W. Minich, N. T. Porile, R. P. Scharenberg, B. C. Stringfellow, and F. Turkot, Phys. Rev. Lett. **49**, 1321 (1982).
[10] A. S. Hirsch, A. Bujak, J. E. Finn, L. J. Gutay, R. W. Minich, N. T. Porile, R. P. Scharenberg, B. C. Stringfellow, and F. Turkot, Phys. Rev. C **29**, 508 (1984).
[11] Sa Ben-Hao and D. H. E. Gross, Nucl. Phys. **A437**, 643 (1985).
[12] J. Bondorf, R. Donangelo, I. N. Mishustin, and H. Schulz, Nucl. Phys. **A444**, 460 (1985).
[13] Zheng Yu-Ming, H. Massmann, Xu Shu-Yan, D. H. E. Gross, Zhang Xiao-Ze, Lu Zhao-Qi, and Sa Ben-Hao, Phys. Lett. B **194**, 183 (1987).
[14] D. H. E. Gross, Yu-Ming Zheng, and H. Massmann, Phys. Lett. B **200**, 397 (1988).
[15] G. Fai and J. Randrup, Nucl. Phys. **A487**, 397 (1988).
[16] Sa Ben-Hao, Zheng Yu-Ming, and Zhang Xiao-Ze, Nucl. Phys. **A509**, 499 (1990).
[17] Sa Ben-Hao, Zheng Yu-Ming, and Zhang Xiao-Ze, Int. J. Mod. Phys. A **5**, 843 (1990).
[18] D. Fabris *et al.*, Phys. Lett. B **196**, 429 (1987).
[19] C. A. Ogilvie *et al.*, Phys. Rev. Lett. **67**, 1214 (1991).
[20] J. Hubele *et al.*, Phys. Rev. C **46**, R1577 (1992).
[21] P. Kreutz *et al.*, Nucl. Phys. **A556**, 672 (1993).
[22] A. S. Botvina and I. N. Mishustin, Phys. Lett. B **294**, 23 (1992).
[23] H. W. Barz, W. Bauer, J. P. Bondorf, A. S. Botvina, R. Donangelo, H. Schulz, and K. Sneppen, Nucl. Phys. **A561**, 466 (1993).
[24] Bao-An Li, A. R. DeAngelis, and D. H. E. Gross, Phys. Lett. B **303**, 225 (1993).
[25] Y. M. Zheng, J. Richert, and P. Wagner, J. Phys. G **22**, 505 (1996).
[26] Zheng Yu-Ming, Wang Fei, Sa Ben-Hao, and Zhang Xiao-Ze, Phys. Rev. C. **53**, 1868 (1996).
[27] Sa Ben-Hao, Zheng Yu-Ming, and Zhang Xiao-Ze, Phys. Rev. C **40**, 2680 (1989).
[28] Chih Ta-Hai, Sa Ben-Hao, Zhang Xiao-Ze, and Zheng Yu-Ming, Phys. Rev. C **42**, 2187 (1990).
[29] Zheng Yu-Ming, Chih Ta-Hai, Li Wen-Xin, Zhang Xiao-Ze, and Sa Ben-Hao, Chin. J. Nucl. Phys. **14**, 116 (1992).
[30] Li Wen-Xin, Sun Tong-Yu, Chih Ta-Hai, Li Yun-Sheng, Zheng Yu-Ming, Sun Ru-Ling, Zhao Li-Li, Wu Ding-Qing, Jing Gen-Ming, and Sa Ben-Hao, Phys. Rev. C **48**, 628 (1993).
[31] Zhang Xiao-Ze, D. H. E. Gross, Xu Shu-Yan, and Zheng Yu-Ming, Nucl. Phys. **A461**, 641 (1987); **461**, 668 (1987).
[32] Y. M. Zheng, S. Y. Xu, X. Z. Zhang, and D. H. E. Gross, Chin. Phys. **10**, 146 (1990).
[33] X. Campi, J. Phys. A **19**, L917 (1986).
[34] H. R. Jaqaman and D. H. E. Gross, Nucl. Phys. **A524**, 321 (1991).
[35] Sa Ben-Hao, Liu Hong-Min, Zheng Yu-Ming, Lu Zhong-Dao, and Zhang Xiao-Ze, J. Phys. G **21**, 241 (1995).
[36] K. Hagel *et al.*, Phys. Rev. Lett. **68**, 2141 (1992).
[37] Sa Ben-Hao, Nucl. Phys. **A499**, 480 (1989).
[38] J. Pochodzalla *et al.*, Phys. Rev. Lett. **75**, 1040 (1995).